ISSN 1054-660X, Laser Physics, 2007, Vol. 17, No. 2, pp. 1–5.

Interferometric Measurement of the Atomic Dipole Phase for the Two Electronic Quantum Paths Generating High-Order Harmonics[1]

A. Pirri[a], C. Corsi[a], E. Sali[a, b], A. Tortora[a, c], and M. Bellini[a, c]

[a] *LENS, Via Nello Carrara 1, 50019 Sesto Fiorentino, Florence, Italy*

[b] *Physics Dept., University of Florence, Via Sansone 1, 50019 Sesto Fiorentino, Florence, Italy*

[c] *Istituto Nazionale di Ottica Applicata, L. go E. Fermi, 6, I-50125, Florence, Italy*

e-mail: pirri@lens.unifi.it

Received September 1, 2006

Abstract—The first direct measurement of the atomic dipole phase in high-order harmonic generation obtained by an interferometric technique in the extreme ultraviolet (XUV) is reported. The effects associated with both the main quantum paths involved in the emission of a given plateau harmonic are investigated and compared with the expectations of the semi-classical model, which offers a very simple physical picture for the understanding of the involved electronic dynamics.

PACS numbers:

DOI: 10.1134/S1054660X0702@@@@

INTRODUCTION

In recent years, many experimental and theoretical studies have significantly improved the knowledge of the physical mechanisms underpinning high-order harmonic generation (HHG) [1], a highly nonlinear process generating coherent radiation in the XUV wavelength range. However, the coherence properties of harmonic radiation are severely influenced by several factors, connected both to single-atom response and to propagation effects in the dispersive (either neutral or partially ionized) gaseous medium. Consequently, in order to use the harmonic radiation either as a coherent source for spectroscopic applications in the XUV region [2, 3] or as an attosecond source of isolated or regularly spaced pulses [4, 5], the ability to control each experimental parameter which can influence the coherence of the HHG process is an essential requirement.

At low gas density and negligible ionization, experimental results have demonstrated that harmonics in the plateau are characterized by a high degree of temporal [6, 7] and spatial coherence [8]. However, also in this case, an intrinsic phase modulation related to the single-atom response, the so-called *atomic dipole phase*, is always present. This effect has long been predicted [9, 10], and the theoretical expectations were experimentally verified by Bellini et al. [6] by investigating the temporal coherence of harmonics. The experiment consisted in studying the far-field interference fringes of high-order harmonics generated by two spatially separated and phase-locked pump pulses. The interference pattern showed a small central zone of high brightness and long coherence time and a less intense surrounding halo with a short coherence time.

Although harmonic generation is a quite complicated issue and a full quantum calculation is required to get a satisfactory simulation of the real process, an intuitive understanding of the physical mechanism can be obtained with a simplified model where the motion of electrons in an external laser field is treated in a classical way. Highly energetic harmonic photons are emitted when the electrons accelerated in the laser field after tunnel ionization return to the parent ion and recombine. According to the strong-field approximation (SFA) [9–12], for a given harmonic in the plateau, only two of the possible electronic trajectories, namely, the "*long*" (*l*) and the "*short*" (*s*) classical ones, give a contribution to the total atomic dipole as

$$d_n(I) = A_n^l(I)\exp(-i\varphi_n^l) + A_n^s(I)\exp(-i\varphi_n^s), \quad (1.a)$$

where

$$\varphi_n^{l,s} = -\alpha_n^{l,s} I(r, t) \quad (1.b)$$

and $A_n^{l,s}$ is the amplitude of the *l* and *s* dipole components, respectively, for the harmonic of order n, while $I(\mathbf{r}, t)$ stands for the space- and time-dependent intensity of the driving field.

The phase $\varphi_n^{l,s}$ linearly depends on the laser intensity through the coefficients $\alpha_n^{l,s}$, which are expected to be approximately proportional to the time that the electrons spend in the continuum along the long or short trajectory, also called the *return time*, before recombination with the parent ion occurs. The return time of the

[1] Paper 5.4.2 presented at the Lausanne LPHYS'06 workshop.

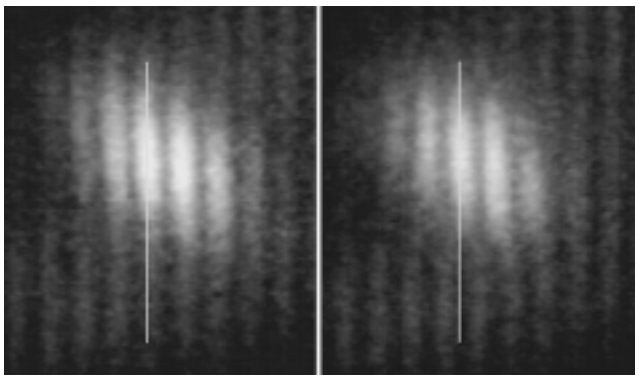

Fig. 1. Interference fringes observed for the 15th harmonic generated in argon for two different conditions of intensity unbalance δI between the two pump pulses. The bright central zone is related to the short quantum path, while the external region derives from the long one. **Left:** when $\delta I = 0$, no relative fringe shift is observed between the two zones. **Right:** when $\delta I \sim 3 \times 10^{13}$ W/cm^2, a relative shift of about half a fringe is observed.

l trajectory is around a full period of the laser, while the other is less than half a period, but they tend to approach each other while going to higher harmonic orders toward the cutoff. The different phase sensitivity of the two components of harmonic emission on the laser intensity has important effects: the transverse spatial variation of the laser intensity imposes different curvatures on the phase fronts (i.e., spatial divergence) of harmonic radiation, while the temporal variation in the laser pulse produces a different time-dependent phase variation (i.e., chirp). Radiation coming from the *s* path is almost not chirped and is well collimated, while that coming from the *l* path is strongly chirped and spatially defocused.

The main goal of our experiment is the direct measurement of the atomic dipole phase coefficients $\alpha_n^{l,s}$ by studying the shift of XUV interference fringes as a function of laser intensity [13]. Two phase-locked pulses are focused in two nearby positions in a gas-jet where two independent harmonic pulses are generated. One of the two pulses is used as a fixed phase reference, while the generating intensity of the other one is changed. According to Eq. (1.b), by changing the laser intensity, the harmonic phase is shifted by

$$\delta\varphi_n^{l,s} = -\alpha_n^{l,s}\delta I. \quad (2)$$

This effect produces a shift in both regions of the XUV interference pattern (the outer region fringes moving faster than the inner ones), which is related to the dipole phase coefficients for the *l* and *s* trajectory of any given harmonic. The relative phase shift between the two regions allows one to measure the difference of the two phase coefficients for the two trajectories by

$$\Delta\varphi_n^{l,s} = (\delta\varphi_n^l - \delta\varphi_n^s) = -(\alpha_n^l - \alpha_n^s)\delta I = -\Delta\alpha_n^{l,s}\delta I. \quad (3)$$

Given the knowledge of both $\alpha_n^{l,s}$, and $\frac{\alpha^l}{\alpha^s}$, one can also extract the values of the nonlinear coefficients by solving the system for the unknown variables. The ratio of the two coefficients can be simply calculated by assuming that the harmonic radiation has a Gaussian shape, linearly chirped by the dipole phase effect. In this case, the coherence time of the linearly chirped harmonic pulses is closely connected to the corresponding dipole coefficient, and the ratio can be simply expressed as

$$\frac{\alpha^l}{\alpha^s} = \frac{\tau_c^s}{\tau_c^l}\sqrt{\frac{\tau_H^2 - (\tau_c^s)^2}{\tau_H^2 - (\tau_c^l)^2}}, \quad (4)$$

where τ_H and $\tau_c^{l,s}$ are the transform-limited harmonic pulse duration and the corresponding coherence time for the long and short trajectory, respectively.

EXPERIMENTAL SETUP

A schematic experimental setup is shown in Fig. 1. An amplified Ti:Sapphire laser system delivering up to 1 mJ pulses with 30-fs time duration at a repetition rate of 1 kHz and centered around 800 nm is used.

The fundamental beam is sent to a partially monolithic Michelson interferometer (which reduces the mechanical instabilities affecting the accuracy of the measurements), where it is divided into two parts by a 50/50 beam splitter. Both the relative delay between the two pulses and their relative intensity can be varied. The first one is regulated close to zero by a computer-controlled stepping motor allowing tiny translations of one of the folding mirrors. The second one is changed by a combination of a quarter-wave plate and a cube polarizer: the former is placed between the beam splitter and one of the two folding mirrors of the interferometer and acts as a half-wave plate upon double passage; the latter selects a common linear polarization for the two pulses copropagating after the interferometer. A rotation of the plate by means of a computer-controlled actuator allows the energy of one of the two pulses to be decreased in a precise way while keeping the other one fixed. The two beams coming from the interferometer are apertured down to a diameter of about 12 mm with an iris and focused by a parabolic mirror of focal length 25 cm into a freely expanding pulsed gas jet. The laser focus is positioned directly under the gas nozzle in order to achieve simultaneous phase-matching conditions for both quantum trajectories and thus to obtain similar intensities for the two harmonic components. Due to the small angle introduced between the two beams coming from the interferometer, they get focused into two different spatial positions of the jet but still quite close to each other and symmetrically placed with respect with the jet axis, so as to interact with a similar gas density. A Pt-Ir normal incidence spherical grating (600 lines/mm) makes a spectral selection of

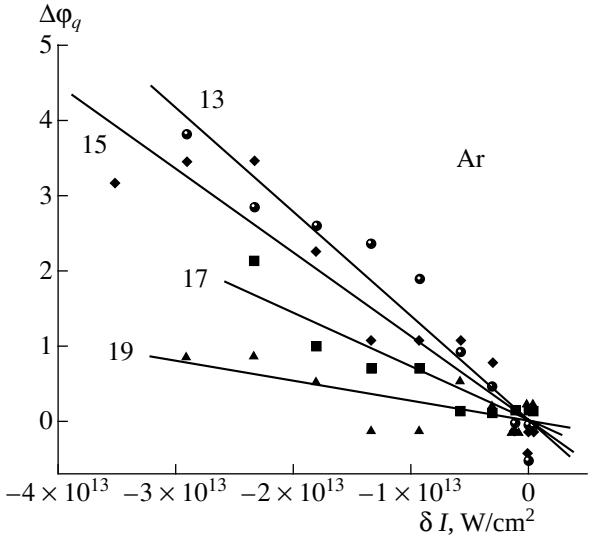

Fig. 2. Measured relative phase shifts between the two regions as a function of the pump intensity unbalance for different harmonic orders.

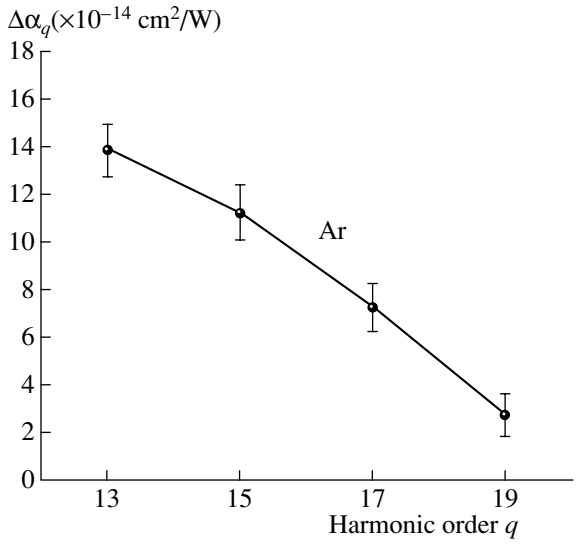

Fig. 3. Measured difference of the nonlinear dipole coefficients for the two electron trajectories.

the two independently generated sources of a given harmonic order and refocuses them onto the plane of the exit slit. As the two XUV pulses start to spatially overlap again upon propagation after this plane, an interference fringe pattern is generated in the far field, which is then detected by an imaging microchannel plate coupled to a phosphor screen (see Fig. 2). The resulting images are finally acquired by a CCD camera and stored on a computer. The exit slit is left completely open, and the fringe patterns are acquired quite far from its plane; therefore, the residual spectral selectivity is completely washed out from the interference patterns. In order to extract information from the fringe interference pattern, two conditions are required: the two harmonic pulses must be independently generated, and the fringe separation must be large enough to be visible. The fringe separation in the far field depends on the distance between the exit slit plane and the detector surface (L), on the harmonic wavelength (λ), and on the distance of the two sources (d) (which is set by the interferometer) as in the formula $\Delta z = \frac{L\lambda}{d}$. As a consequence, the distance between the two beams should be made small in order to have a sufficient fringe separation on the detector. On the other hand, the two harmonic beams can be considered independent only if the distance between the two foci is bigger than their waist diameter. We have measured the beam waist radii and the separation between the beam centers at the focus finding about 20 μm and 60 μm, respectively. In such conditions, both requirements described above are fulfilled, and fringe separations on the order of 0.5 mm are obtained for all the harmonic orders investigated. With a mean laser power of about 48 mW per beam, we have estimated a peak intensity of about 1.2×10^{14} W/cm^2 in the focal spot of each of the two pulses. It is important to emphasize that this laser intensity is chosen to be well below the saturation intensity of argon (the gas used for harmonic generation at a backing pressure of about 1.8 bar), thus making ionization effects in the process totally negligible and allowing us to assume that harmonics are always generated close to the peak of the driving laser pulse.

RESULTS AND DISCUSSION

Figure 1 reports the interference fringes for the 15th harmonic generated in argon at zero relative time delay between the two pump pulses, when equal intensity (left, $\delta I = 0$) and unequal intensity (right, $\delta I \neq 0$) are used to generate the two harmonics. The presence of the two regions predicted by the semi-classical model allows us to measure the relative fringe shifts of the harmonics, $\Delta\varphi_n^{l,s}$, as a function of the unbalance between the laser intensity of the two pump pulses coming from the Michelson interferometer. The measurement of the relative phase shifts, instead of the absolute ones for the two regions separately, avoids the detrimental effects of the residual instabilities of the interferometer and also eliminates all possible spurious phase shifts introduced in the measurements.

According to Eq. (3), the measured phase difference for all harmonics in the plateau should show a linear dependence on the laser intensity unbalance, which is clearly seen in the experiments (see Fig. 2, where the solid lines represent the linear fits). The trend of the corresponding slope of the phase difference curves is plotted in Fig. 3. It decreases for increasing harmonic orders and tends to vanish when approaching the cutoff region. This behavior is closely related to the trend of

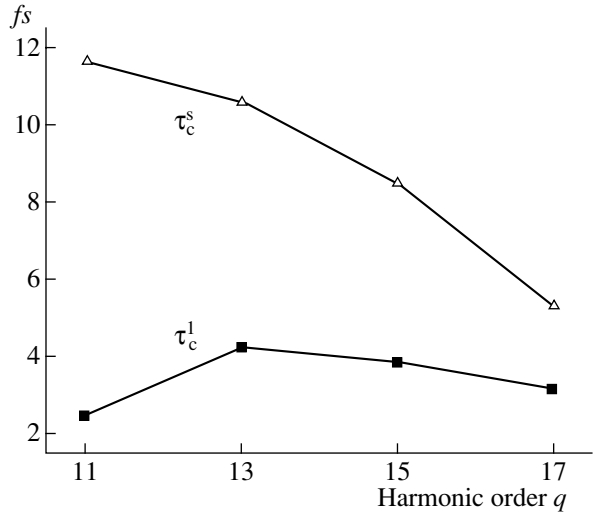

Fig. 4. Measured coherence times for the long and the short electron trajectories.

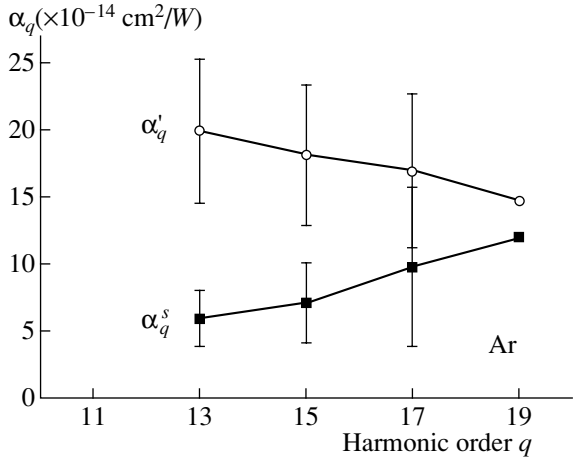

Fig. 5. Experimentally derived values for the atomic dipole coefficients. Data points for the 19th harmonic are obtained by placing them at the measured relative distance around the mean of the data obtained for the 17th harmonic.

the return times characterizing each electron trajectory. As expected in the SFA approximation, the difference in the dipole coefficients $\Delta\alpha_n^{l,s}$ is roughly proportional to the difference between the return times for the two trajectories. This difference is large for harmonics in the plateau, while it gets smaller when moving toward the cutoff region.

By using the same experimental apparatus, we have also estimated the harmonic coherence time which, mathematically speaking, corresponds to the half-width at half-maximum of the curve representing the fringe visibility as a function of the delay. The visibility curve is obtained by changing the relative delay of the two equal-intensity pump pulses and recording the contrast of the fringe pattern for both the two zone corresponding to the *long* and *short* quantum paths.

In Fig. 4, the measured coherence times for different harmonic orders are reported. The inner and outer regions are clearly characterized by two different coherence times. By increasing the delay between the laser pulses, the interference fringes of the inner region slowly disappear: this corresponds to a long coherence time which is seen to decrease rapidly with increasing harmonic orders (roughly from about 12 fs for the 11th to 5 fs for the 17th). In contrast, the interference fringes of the outer region disappear very quickly with the delay, showing a short coherence time which increases slightly with harmonic order.

Figure 5 reports the final results for the dipole phase coefficients as a function of the harmonic order which have been calculated using Eqs. (3) and (4) assuming a harmonic time duration of about 15 fs. The experimental data present the behavior expected from the simple semi-classical model and are in good agreement with previous experimental data [14–18] and with theoretical calculations [19–22]. It should be noted that all the previous measurements of dipole phase coefficients in HHG have been performed by making use of the fact that the time variation of the laser pulse intensity induces a frequency chirp on the harmonics. A measurement of the harmonic chirp for only one of the two electronic trajectories, together with other assumptions, thus allows the dipole phase coefficients to be inferred. Here, for the first time, a direct interferometric method is used as the most natural way to measure phases, and both quantum paths are analyzed at the same time.

CONCLUSIONS

We have reported the first direct measurements of the dipole phase in HHG by XUV interferometry. This approach allowed us to analyze the contribution of each electronic quantum path by the observation of fringe shifts in the interference pattern of the harmonics. Experimental data show a good agreement with the semi-classical model, which allows one to understand the electronic dynamics involved in the HHG process by using a simple physical picture. Moreover, data are in good agreement with other measurements based on the analysis of the frequency chirp of harmonic pulses. The knowledge and the control of these processes is a crucial point for XUV interferometric and spectroscopic applications, as well as for attosecond pulse generation.

REFERENCES

1. P. B. Corkum, Phys. Rev. Lett. **71**, 1994 (1993).
2. S. Cavalieri et al., Phys. Rev. Lett. **89**, 133002 (2002).
3. S. Witte et al. Science **307**, 400 (2005).
4. Hentschel et al. Nature **413**, 509 (2001).
5. P. M. Paul et al. Science **292**, 1689 (2001).
6. M. Bellini et al., Phys. Rev. Lett. **81**, 297 (1998).

7. C. Lynga et al., Phys. Rev. A **60**, 4823 (1999).
8. T. Ditmire, Phys. Rev. Lett. **77**, 4756 (1996).
9. P. Salieres et al., Phys. Rev. Lett. **74**, 3776 (1995).
10. L. Lewenstein, P. Salieres and A. L'Huillier, Phys. Rev. A **52**, 4747 (1995).
11. W. Becker, S. Long and J.K. Melver, Phys. Rev. A **50**, 1540 (1994).
12. L. Lewenstein, et al., Phys. Rev. A **49**, 2117 (1994).
13. C. Corsi et al., Phys. Rev. Lett. **97**, 23901 (2006).
14. P. Salieres et al., Science **292**, 902 (2001).
15. Y. Mairesse et al., Phys. Rev. Lett. **94**, 173903 (2005).
16. E. Benedetti et al., Opt. Express **14**, 2242 (2006).
17. J. Mauritsson et al., Phys. Rev. A **70**, 021801 (2004).
18. T. Sekikawa, T. Kanai and S. Watanabe, Phys. Rev. Lett. **91**, 103902 (2003).
19. M. B. Gaarde et al. Phys. Rev. A **59**, 1367 (1999).
20. M. B. Gaarde Opt. Express **58**, 529 (2001).
21. K. J. Schafer, Phys. Rev. A **65**, 031406 (2002).
22. J. H. Kim et al. Phys. Rev. A **63**, 063403 (2001).

SPELL: OK